Nuclear Materials and Energy 18 (2019) 18–22

Contents lists available at ScienceDirect

Nuclear Materials and Energy

journal homepage: www.elsevier.com/locate/nme

The adhesion of tungsten dust on plasma-exposed tungsten surfaces

P. Tolias*[a], M. De Angeli[b], G. Riva[c], S. Ratynskaia[a], G. Daminelli[c], L. Laguardia[b], M. Pedroni[b], D. Ripamonti[c], A. Uccello[b], E. Vassallo[b]

[a] Space and Plasma Physics - KTH Royal Institute of Technology, Teknikringen 31, 10044 Stockholm, Sweden
[b] Istituto di Fisica del Plasma - Consiglio Nazionale delle Ricerche, via Cozzi 53, 20125 Milan, Italy
[c] Institute of Condensed Matter Chemistry and Energy Technologies - Consiglio Nazionale delle Ricerche, via Cozzi 53, 20125 Milan, Italy

ARTICLE INFO

Keywords:
Dust adhesion
Pull-off force
Dust remobilization
Electrostatic detachment
Adsorbates
Sputtering

ABSTRACT

The adhesion of tungsten dust is measured on plasma-exposed and non-exposed tungsten substrates with the electrostatic detachment method. Tungsten substrates of comparable surface roughness have been exposed to the deuterium plasmas of the GyM linear device and the argon plasmas of rf glow discharges under conditions which invariably modify the surface composition due to physical sputtering. The adhesion has been systematically characterized for different spherical nearly monodisperse dust populations. Independent of the dust size, an approximate 50% post-exposure reduction of the average and spread of the adhesive force has been consistently observed and attributed to surface chemistry modifications.

1. Introduction

The adhesion of tokamak dust on plasma-facing components emerges in various theoretical topics (mechanical impacts, plasma induced remobilization, resuspension during loss-of-vacuum accidents) and diagnostic issues (collection activities, removal techniques) [1–6]. This motivated systematic pull-off force measurements utilizing the electrostatic detachment method [7,8] and dedicated van der Waals calculations employing Lifshitz theory [9]. The experimental investigations focused on micron sized spherical tungsten dust deposited in a controlled manner on tungsten substrates of low surface roughness ($\lesssim$100 nm). Their principal conclusions can be summarized in the following: **(i)** The W-on-W adhesive force has an average value that is nearly two orders of magnitude smaller than the predictions of contact mechanics but in good agreement with the van der Waals formula. Intimate contact is restricted due to the omnipresent nano-roughness implying that adhesion is dominated by interactions between instantaneously induced multipoles and not by metallic bonding. **(ii)** The W-on-W adhesive force approximately behaves as a log-normally distributed random variable. The statistical character of surface roughness, adsorbate coverage and micro-crystallite orientation leads to the stochastic nature of adhesion. **(iii)** Gas-assisted deposition (mimicking dust sticking to the first wall and divertor) leads to stronger adhesion than gravity-assisted deposition (mimicking dust sticking to the vessel floor) as a result of plastic deformation realized even during low velocity impacts. **(iv)** The presence of thin beryllium coatings on W surfaces does not significantly modify the adhesion of W dust.

In addition to these qualitative results, empirical correlations were proposed which describe the dust size dependence of the mean as well as the spread of the W-on-W adhesive force in specific surface roughness ranges [8]. In combination with the log-normal distribution, these correlations provide a complete analytic description of W-on-W adhesion. The pertinent question that arises concerns whether quantitative results obtained in the laboratory can be expected to be accurate in the tokamak environment given the well-known dependence of adhesion on surface composition [10]. The aforementioned measurements were carried out in a low pressure chamber and standard surface precleaning techniques were followed, *i.e.* degreasing in deionised water followed by ultrasonic baths in turpentine and acetone for several minutes. As a result of the absence of ultra-high vacuum conditions and *in situ* cleaning provisions (*e.g.* inert gas sputtering or self-sputtering), the W substrates were not atomically clean but rather contained adsorbates and native oxides. Thus, the measurements must have been subject to chemical heterogeneities affecting the mean and spread of the adhesive forces.

The purpose of this work is to quantify the effect of typical atmospheric contaminants on W-on-W adhesion. This is indirectly achieved by exposing dust-free W substrates to plasma discharges, under conditions which invariably modify the surface chemistry by physical sputtering. Post exposure, the sputter-cleaned substrate is returned to the ambient environment, dust is deposited and electrostatic detachment measurements are carried out. Inevitably, the plasma-exposed substrate

* Corresponding author.
E-mail address: tolias@kth.se (P. Tolias).

https://doi.org/10.1016/j.nme.2018.12.002
Received 24 July 2018; Received in revised form 29 November 2018; Accepted 1 December 2018

will be gradually covered again with adsorbates, but the pull-off force is measured before the original surface chemistry is completely re-established. More important, this experimental sequence follows the chain of events occurring in loss-of-vacuum accidents, during which air ingress in the vacuum vessel generates an outward flow after pressure equilibration that can potentially mobilize adhered dust grains [11,12].

2. Experimental aspects

2.1. Electrostatic detachment method

Here, we shall briefly present the operation principle of the measurement technique and the main stages of the experimental procedure. For further theoretical and technical details, the reader is referred to our previous works [7,8].

In the electrostatic detachment method [13], a dc potential difference is applied between two parallel plate electrodes with the conducting dust deposited on the grounded electrode. The interaction between this electrostatic field and the induced dust charge leads to a normal force that tends to detach the grains from the substrate. For the idealized spherical dust - planar substrate system, its magnitude is described by the Lebedev formula [14]

$$F_e = k_D E^2 D_d^2 \ (\mu N), \tag{1}$$

where E is the electrostatic field in kV/mm, D_d the dust diameter in μm and $k_D = 0.38 \times 10^{-4}\,(\mu N mm^2)/(kV^2 \mu m^2)$. The adhesive force or pull-off force F_{po} can be measured by slowly increasing the bias until the detachment condition $F_e \geq F_{po}$ is satisfied. Owing to the omnipresent structural heterogeneities (different surface topology), chemical heterogeneities (variable adsorbate composition or content) and energetic heterogeneities (random microcrystallite orientation) of the dust-substrate system, complete detachment does not occur above a unique electric field strength but gradual detachment occurs over an extended range of electric fields. Hence, the method provides a measurement of the cumulative distribution function $\Phi(F_{po})$ of the random variable F_{po}, whose average value and standard deviation can then be straightforwardly computed.

In our experiments, three nearly monodisperse spherical W dust batches (6 μm, 9 μm, 14 μm) were meshed out from a wide 5–25 μm population supplied by TEKNA Advanced Materials Inc. Each dust subpopulation was adhered to W substrates with gravity-assisted deposition [8]. These dust-loaded substrates were adjusted into a hollow stainless steel electrode which was mounted as the bottom electrode of the low pressure (< 0.05 Pa) high-voltage system, whereas the upper electrode was kept dust-free. A 1.5 kV potential difference was initially applied and maintained constant for several minutes. The vacuum was then broken, the bottom electrode was dismounted and the mobilized dust number was determined by an optical microscope. The procedure was repeated with a slightly higher bias until all dust had been removed or dielectric breakdown had occurred. Clusters were excluded from counting. With 1.5–25 kV biases and 0.5–1 mm electrode spacings, E = 1.5–50 kV/mm extracting fields were achieved.

2.2. Plasma exposures

Dust-free W substrates of similar surface roughness characteristics were exposed to the deuterium plasma of the GyM linear device and the argon plasma of an rf glow discharge. The samples were negatively biased with respect to the plasma in order to warrant that physical sputtering is realized. For the sake of clarity, we emphasize again that only dust-free and not dust-adhered W substrates were exposed to plasmas to ensure that the - otherwise shadowed - contact area is plasma wetted but also to avoid possible contact strengthening due to diffusion bonding at elevated temperatures.

GyM deuterium exposures. The device and the sample introduction system are described in Refs. [15–17]. The plasma parameters at the center of the column were measured with a Langmuir probe. **(a)** Two W substrates (#1, #4) were exposed under the conditions: $n_e \simeq 5.2 \times 10^{16}$ m^{-3} for the plasma density, $T_e \simeq 6.0$ eV for the electron temperature, $V_p \simeq 15$ V for the plasma potential, $V_b = -400$ V for the applied sample bias, $t_{exp} \simeq 90$ min for the exposure time and $F_i \simeq 2.9 \times 10^{24}$ m^{-2} for the ion fluence. The incident ions were monoenergetic ($T_i \sim 0.1$ eV) with a kinetic energy of $E_{inc} = e(V_p - V_b)$. The normal incidence sputtering yield was found to be $Y_{D\rightarrow W}(E_{inc}) \simeq 8.1 \times 10^{-4}$ from the Eckstein–Preuss empirical formula [18,19]. This estimate neglects the presence of surface roughness (leading to a Y increase due to the more grazing ion incidence), the possibility of self-sputtering by promptly ionized W atoms (leading to a contribution that depends on the ionization efficiency with $Y_{W\rightarrow W}(E_{inc}) \simeq 0.44$), the possibility of sputtering by oxygen impurities [20] (leading to another contribution that depends on the concentration with $Y_{O\rightarrow W}(E_{inc}) \simeq 0.24$) and the presence of deuterium molecules in the plasma beam (leading to an effective F_i decrease due to the constituent's kinetic energy $E_{inc}/2$ lying below the sputtering threshold). The W erosion depth was then calculated as $s = [F_i Y_{D\rightarrow W}(E_{inc}) m_{at}]/\rho_m$, where m_{at} is the W atomic mass and ρ_m the W mass density, resulting to $s \sim 40$ nm. The temperature of the sample holder reached $T_{fin} \simeq 380$ °C at the end of each exposure. **(b)** One W substrate (#5) was exposed under the conditions: $n_e \simeq 5.3 \times 10^{16}$ m^{-3}, $T_e \simeq 6.2$ eV, $V_p \simeq 16$ V, $V_b = -100$ V, $t_{exp} \simeq 90$ min, $F_i \simeq 3.0 \times 10^{24}$ m^{-2}, $T_{fin} \simeq 270$ °C. As a consequence of the lower applied bias, the incident kinetic energy was much smaller than the D → W sputtering threshold of $E_{th} \simeq 230$ eV [19] and thus there could be no material removal due to sputtering by deuterium ions.

Rf glow discharge argon exposures. The discharge consists of two stainless steel parallel capacitive-coupled plate electrodes, mounted inside a cylindrical vacuum chamber, in an asymmetric configuration. The powered electrode is connected to a 13.56 MHz rf power supply, coupled to an automatic impedance matching unit, while the other electrode is grounded. The exposed samples were mounted on the grounded electrode. Two W substrates (#2, #3) were exposed under the conditions: $n_e \simeq 2.5 \times 10^{14}$ m^{-3}, $V_b = -230$ V, $t_{exp} \simeq 25$ min and $F_i \simeq 10^{21}$ m^{-2}. The substrates remained close to room temperature during the exposures. As a result of the larger argon atomic mass, the Ar → W sputtering threshold is much smaller, $E_{th} \simeq 27$ eV [19], and modest sputtering still takes place in spite of the smaller applied bias and ion fluence. The normal incidence sputtering yield was found to be $Y_{Ar\rightarrow W}(E_{inc}) \simeq 0.33$ from the Eckstein–Preuss empirical formula and the erosion depth was estimated to be $s \sim 5$ nm.

Substrate analysis. The dust deposition areas of each W substrate were observed before and after plasma exposure by means of a scanning electron microscope (SEM) in order to ensure that the substrate morphology remained the same. In addition, the surface roughness of each sample was measured before and after plasma exposure by means of atomic force microscopy (AFM). Finally, qualitative information on the adsorbate composition of the substrate was obtained before and after plasma exposure by means of Attenuated Total Reflection Fourier Transform Infra-Red (ATR-FTIR) spectroscopy.

3. Experimental results

3.1. Pull-off force measurements

In all 25 measurement sets, the W-on-W adhesive force approximately behaved as a log-normally distributed random variable [8,21,22], see Figs. 1 and 2 for some characteristic examples. The average value and the standard deviation (spread) of the pull-off force were calculated from

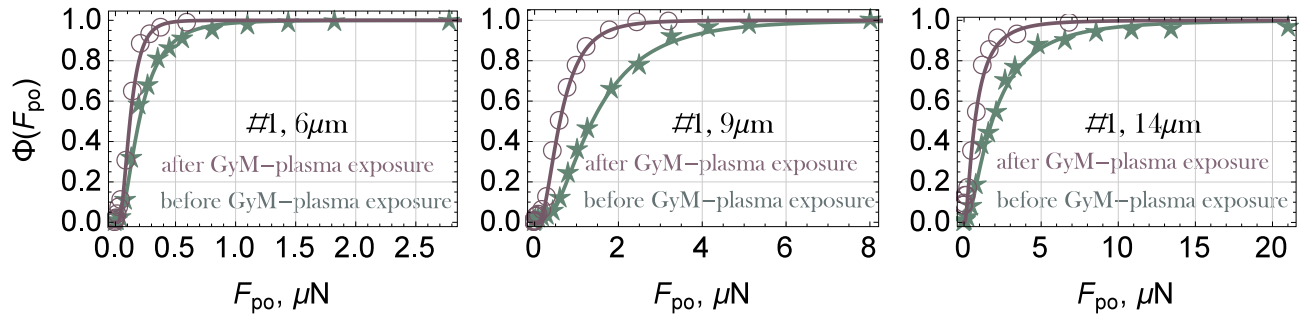

Fig. 1. The experimental cumulative probability distribution of the W-on-W adhesive force (discrete points) together with the least-square fitted log-normal cumulative probability (solid line). Measurements for W dust deposited before and after W substrate exposure to the GyM deuterium plasma. Results for substrate #1: $D_{\text{nom}} = 6\,\mu$m, $D_{\text{nom}} = 9\,\mu$m and $D_{\text{nom}} = 14\,\mu$m.

$$\bar{F}_{\text{po}} = \sum_{i=1}^{M}\left[\left(\frac{N_i}{N}\right)F_{\text{e},i}\right] \Big/ \sum_{i=1}^{M}\left(\frac{N_i}{N}\right), \tag{2}$$

$$\sigma[F_{\text{po}}] = \sqrt{\sum_{i=1}^{M}\left[\left(\frac{N_i}{N}\right)(F_{\text{e},i} - \bar{F}_{\text{po}})^2\right] \Big/ \sum_{i=1}^{M}\left(\frac{N_i}{N}\right)} \tag{3}$$

where M is the number of distinct electrostatic field values, N is the total number of adhered dust grains, N_i is the number of dust grains detached by the ith applied electrostatic field E_i, $F_{\text{e},i} = k_{\text{D}}E_i^2D_{\text{d,av}}^2$ is provided by the Lebedev formula which is evaluated at the average adhered dust diameter $D_{\text{d, av}}$. The denominator is not necessarily unity, since dielectric breakdown can take place prior to the detachment of all adhered dust grains [7,8]. The experimental results have been summarized in Table 1.

Substrates #1, 2, 3. Pull-off force measurements were carried out with the 6, 9, 14 μm W dust batches deposited on the substrates before and after their plasma exposure. The substrates were subject to physical sputtering during exposure. A significant post-exposure reduction of the average and spread of the pull-off force was always observed regardless of the dust diameter. For the 6 μm subpopulation, the $\bar{F}_{\text{po}}$ reduction ranged from 45 to 76 and the $\sigma[F_{\text{po}}]$ reduction from 54 to 66%. For the 9 μm subpopulation, the $\bar{F}_{\text{po}}$ reduction ranged from 20 to 57% and the $\sigma[F_{\text{po}}]$ reduction from 32 to 60%. For the 14 μm subpopulation, the $\bar{F}_{\text{po}}$ reduction ranged from 41 to 54% and the $\sigma[F_{\text{po}}]$ reduction from 43 to 48%. It can be roughly stated that plasma exposure of the substrates led to a 50% reduction in the average and spread of the adhesive force with no apparent dependence on the dust size.

Substrate #4. Pull-off force measurements were performed with the 6, 9, 14 μm W dust batches deposited on the substrate right after and nearly two months after (remaining in atmospheric environment) its plasma exposure. The substrate was also subject to physical sputtering during exposure. The average and spread of the pull-off force were again significantly lower right after plasma exposure: $\bar{F}_{\text{po}}$ was lower by 19%, 39%, 68% and $\sigma[F_{\text{po}}]$ was lower by 29%, 37%, 52% for the 6, 9, 14 μm batches, respectively.

Substrate #5. Pull-off force measurements were carried out with the 14 μm W dust batch deposited on the substrate only right after its plasma exposure. This substrate was not subject to physical sputtering during exposure. The average and spread of the pull-off force acquired values similar to the pre-exposure values of other samples (nearly identical to the #1 substrate).

Pre-exposure measurements. It is important to point out that, despite the nearly identical substrate roughness values, there are large deviations between the pull-off force measurements carried out with different non-exposed substrates. For instance, in the case of substrates #2, 3 (rms roughness $R_{\text{q}} \simeq 15$ and 24 nm): the measurements are very similar for the 9 μm, 14 μm batches but exhibit large differences for the 6 μm subpopulation. In the case of substrates #1, 2 (rms roughness $R_{\text{q}} \simeq 16$ and 15 nm): the measurements are nearly identical for the 9 μm batch, similar for the 14 μm batch but exhibit very large differences for the 6 μm subpopulation. These deviations are, mostly probably, a consequence of chemical heterogeneities (a residual contribution from structural heterogeneities cannot be excluded because identical average roughness metrics for the substrate do not imply an identical surface topology and also because the dust surface roughness may vary). The effect of energetic heterogeneities should be more limited, as suggested from the similar surface energies calculated for different W crystal facets [23]. The possibility of bias due to strong chemical heterogeneities necessitates the use of different substrates and the acquisition of large statistics for reliable pull-off force measurements, as also discussed in Ref. [8].

3.2. Surface chemistry modifications

AFM measurements, focused on the deposition areas, revealed that the plasma exposures barely modified the surface roughness characteristics of the W substrates. For instance, the rms metric R_{q} increased

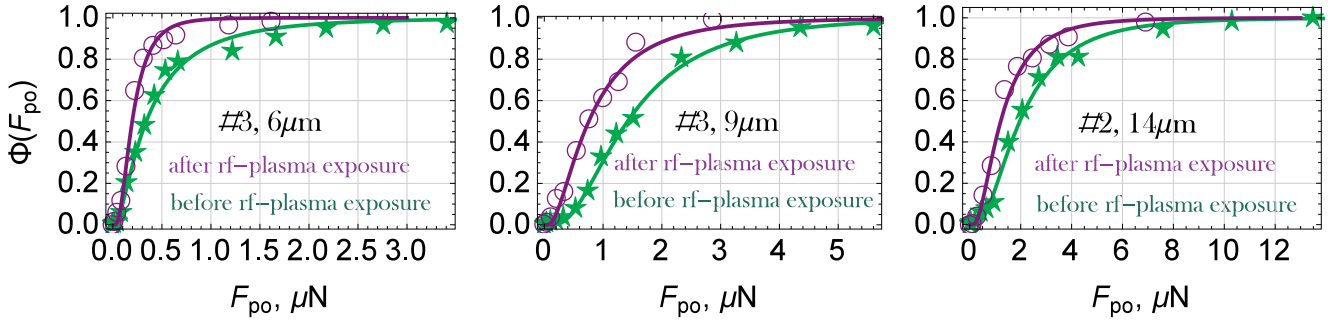

Fig. 2. The experimental cumulative probability distribution of the W-on-W adhesive force (discrete points) together with the least-square fitted log-normal cumulative probability (solid line). Measurements for W dust deposited before and after W substrate exposure to the rf argon plasma. Results for $D_{\text{nom}} = 6\,\mu$m (substrate #3), $D_{\text{nom}} = 9\,\mu$m (substrate #3) and $D_{\text{nom}} = 14\,\mu$m (substrate #2).

Table 1
Summary of pull-off force measurements carried out with the electrostatic detachment method for spherical W dust adhered to W surfaces with gravity-assisted deposition. Total of 25 sets of measurements performed with 5 different substrates and 3 different dust sub-populations. The designation "no plasma" refers to measurements carried out either before substrate exposure to plasmas (#1, #2, #3) or two months after substrate exposure to plasmas (#4). The designation "plasma" refers to measurements carried out right after substrate exposure to plasmas.

Tungsten substrate history	Average W dust diameter (μm) *No plasma*	Number of isolated W dust grains *No plasma*	Average pull-off $\bar{F}_{po}$ (μN) *No plasma*	Pull-off force spread (μN) *No plasma*	Average W dust diameter (μm) *Plasma*	Number of isolated W dust grains *Plasma*	Average pull-off $\bar{F}_{po}$ (μN) *Plasma*	Pull-off force spread (μN) *Plasma*
#1: exposure in GyM D plasma ($V_b = -400$ V)	6.10 9.20 14.9	1742 884 273	0.31 1.99 2.87	0.30 1.44 2.96	6.30 9.10 15.2	1851 937 104	0.17 0.85 1.32	0.10 0.57 1.54
#2: exposure in Ar rf-discharge ($V_b = -230$ V)	5.20 9.39 15.3	1482 855 296	1.18 1.91 3.28	0.65 1.42 2.84	6.20 9.05 14.6	1421 1199 196	0.28 1.54 1.92	0.26 0.96 1.63
#3: exposure in Ar rf-discharge ($V_b = -230$ V)	6.00 9.05 14.4	1199 678 297	0.62 1.87 3.45	0.65 1.13 2.71	5.91 9.18 15.2	1893 783 196	0.32 1.10 1.98	0.30 0.77 1.46
#4: exposure in GyM D plasma ($V_b = -400$ V)	6.50 9.40 15.1	1969 1139 317	0.26 1.35 3.56	0.21 0.81 1.90	6.10 9.00 15.4	1489 1021 291	0.21 0.82 1.13	0.15 0.51 0.91
#5: exposure in GyM D plasma ($V_b = -100$ V)					15.1	339	2.91	2.96

from 16 to 23 nm after the exposure of substrate #1 to the GyM linear device and increased from 24 to 32 nm after the exposure of substrate #3 to the rf glow discharge. We also point out that, at least for $D_d = 5$–25 μm and $R_q \simeq 10 - 100$ nm, a rather weak dependence of the W-on-W adhesive force on surface roughness has been consistently observed [8]. Thus, the effect of topological changes should be negligible. In addition, although elevated in the GyM exposures, the substrate surface temperatures remained well below the W recrystallization temperature range of 1000–1300 °C. Therefore, micro-crystallite restructuring should also be negligible.

On the other hand, the surface composition of the W substrate was strongly modified by plasma exposure due to physical sputtering and possibly also chemical sputtering or thermal desorption of the contaminants (the latter two only possible for the deuterium GyM exposures). Plasma exposure should preferentially remove adsorbates as well as native oxides from the near-surface region leaving a purer but highly reactive W surface. Upon return to the atmospheric environment, the activated substrate would again begin to be covered with adsorbates and slowly re-establish its original surface chemistry. In fact, there are appreciable differences in the ATR-FTIR spectra before and after exposure to the GyM deuterium plasma. Prior to exposure, the spectrum was dominated by vibrational bands ascribed to OH groups, whereas, post exposure, the spectrum became dominated by oxide bands and the OH bands nearly disappeared, see Fig. 3 for a characteristic example. We note, though, that the differences in the ATR-FTIR spectra before and after exposure to the rf argon plasma are much less pronounced.

The above arguments and measurements suggest that the reduction of the average value and spread of the pull-off force after plasma exposure, as observed in the adhesion measurements for substrates #1, 2, 3, was primarily caused by surface chemistry modifications. The interpretation is strongly supported by the adhesion measurements for substrate #4 (where two month subjection to atmospheric conditions led to an increase in both average and spread) but also for substrate #5 (where in absence of physical sputtering there were nearly no changes in the pull-off force characteristics).

From the perspective of the Lifshitz theory of van der Waals forces [24,25], the presence of adsorbates will alter the near-surface dielectric function of the bodies and will thus result to a different

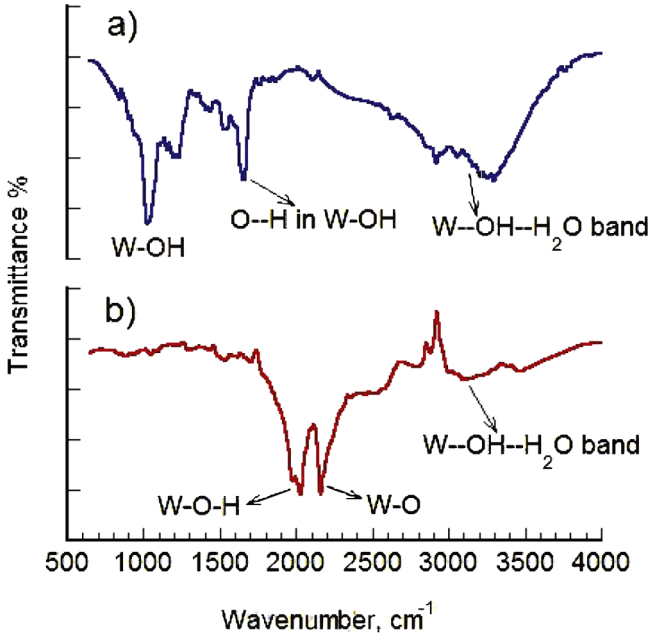

Fig. 3. The ATR-FTIR spectrum of the W substrate #1 before (a) and right after (b) exposure to the deuterium plasma of the GyM linear device. In the post-exposure spectra, H stands for any hydrogen isotope, given the possibility of deuterium retention. The spectra were acquired by a Perkin Elmer Spectrum One FTIR Spectrometer featuring zinc selenide as the high refractive index crystal at a 45° infrared beam incident angle.

Hamaker constant. This is illustrated in Fig. 4, where effective W-on-W Hamaker constants A_{eff} are computed before as well as after plasma exposure and compared with the theoretical pure W-on-W Hamaker constant $A_{the} = 4.98 \times 10^{-19}$ J [9]. In particular, for each dust size, the datasets for substrates #1, 2, 3 have been unified and two $\bar{F}_{po}$ values have been calculated that characterize adhesion before and after exposure. This allows for the least-squares determination of the effective W-on-W Hamaker constant, which is $A_{eff} \simeq 3.93 \times 10^{-19}$ J before and $A_{eff} \simeq 2.22 \times 10^{-19}$ J after exposure.

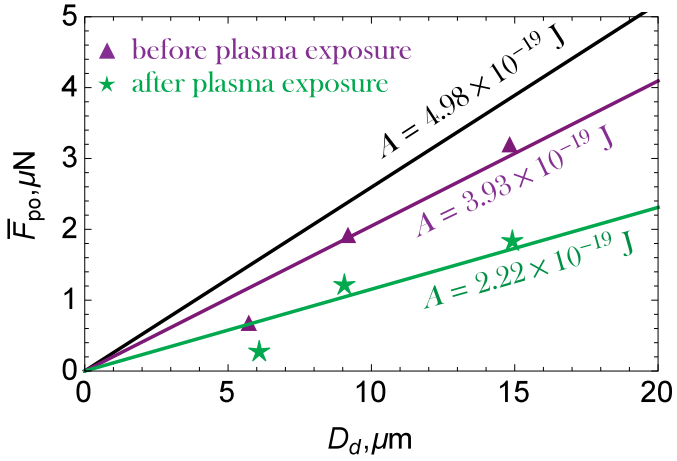

Fig. 4. The average value of the W-on-W adhesive force, before and after plasma exposure under physical sputtering conditions (synthetic dataset constructed by unifying the results acquired for substrates #1, 2, 3), as a function of the dust size. The van der Waals expression $F_{vdW} = [A/(12z_0^2)]D_d$ [24,25] with the distance of closest approach $z_0 = 0.4$ nm [9] and with three different Hamaker constants is also illustrated: (i) the theoretical $A_{the} = 4.98 \times 10^{-19}$ J for pure tungsten, (ii) the least-squares determined $A_{eff} \simeq 3.93 \times 10^{-19}$ J before plasma exposure, (iii) the least-squares determined $A_{eff} \simeq 2.22 \times 10^{-19}$ J after plasma exposure.

4. Summary and discussion

The adhesion of micron-sized tungsten dust has been measured on plasma-exposed and non-exposed tungsten substrates of similar surface roughness characteristics with the electrostatic detachment method. Prolonged substrate exposures were carried out in the deuterium plasmas of the GyM linear device and the argon plasmas of rf glow discharges with large negative biasing in order to ensure that physical sputtering is realized. After substrate exposure, the adhesive force remained log-normally distributed but, nearly independent of the dust size, a roughly 50% reduction of its average and standard deviation was consistently observed. This reduction was attributed to surface composition modifications. In spite of the fact that vacuum was interrupted for the dust deposition and in-between successive electrostatic field applications, the surface chemistry remained distinctly different from the original.

The experimental results quantify the effect of typical atmospheric contaminants on the W-on-W adhesive force. This effect is rather strong, especially when taking into consideration the fact that the presence of thin beryllium coatings (up to 1000 nm) has been demonstrated to only weakly modify the adhesion of W dust [8]. Since it is not possible to perform pull-off force measurements with the electrostatic detachment method in ultra-high vacuum and involving atomically clean W surfaces (substrates and dust), the chemical composition of the surfaces should always be carefully monitored. Under fusion-relevant conditions, helium trapping (bubble, fuzz formation) as well as nitrogen implantation (tungsten nitride formation) lead to a distinct near-surface chemistry [26–28], whose effect on W-on-W adhesion could also be significant. Finally, it is worth noting that tritiated dust will tend to be positively charged due to the emission of beta electrons generated by the radioactive decay of tritium [29,30]. Provided that the electrical resistance at the dust-substrate contact is high enough to sustain the charge surplus within the dust particle, this would not only influence adhesion but also the dust response to external electric fields.

Conflict of interest

The authors declare that they have no known competing financial interests or personal relationships that could have appeared to influence the work reported in this paper.

Acknowledgments

PT would like to acknowledge the financial support of the 2018 CNR Short Term Mobility Program. This work has been carried out within the framework of the EUROfusion Consortium and has received funding from the Euratom research and training programme 2014–2018 under grant agreement no. 633053. Work performed under EUROfusion WP PFC. The views and opinions expressed herein do not necessarily reflect those of the European Commission.

References

[1] S. Ratynskaia, C. Castaldo, H.B. ker, D. Rudakov, Plasma Phys. Control. Fusion 53 (2011) 074009.
[2] A. Shalpegin, F. Brochard, S. Ratynskaia, P. Tolias, Nucl. Fusion 55 (2015) 112001.
[3] P. Tolias, S. Ratynskaia, M. De Angeli, G. De Temmerman, Plasma Phys. Control. Fusion 58 (2016) 025009.
[4] S. Ratynskaia, P. Tolias, I. Bykov, D. Rudakov, Nucl. Fusion 56 (2016) 066010.
[5] S. Peillon, A. Roynette, C. Grisolia, F. Gensdarmes, Fusion Eng. Des. 89 (2014) 2789.
[6] S. Rosanvallon, C. Grisolia, P. Andrew, S. Ciattaglia, J. Nucl. Mater. 390–391 (2009) 57.
[7] G. Riva, P. Tolias, S. Ratynskaia, G. Daminelli, Nucl. Mater. Energy 12 (2017) 593.
[8] P. Tolias, G. Riva, M. De Angeli, S. Ratynskaia, Nucl. Mater. Energy 15 (2018) 55.
[9] P. Tolias, Fusion Eng. Des. 133 (2018) 110.
[10] H.J. Butt, M. Kappl, Surface and Interfacial Forces, Wiley-VCH Verlag, Weinheim, 2010.
[11] H.W. Bartels, A. Poucet, G. Cambi, C. Gordon, Fusion Eng. Des. 42 (1998) 13.
[12] T. Honda, H.W. Bartels, B. Merrill, T. Inabe, Fusion Eng. Des. 47 (2000) 361.
[13] D.W. Cooper, H.L. Wolfe, Aerosol Sci. Technol. 12 (1990) 508.
[14] N.N. Lebedev, I.P. Skalskaya, Sov. Phys. Tech. Phys. 7 (1962) 268.
[15] G. Granucci, D. Ricci, S. Alocci, B. Baiocchi, Proc. 36th EPS Conference on Plasma Physics, June 29–July 3 2009, Sofia, Bulgaria, 33E ECA, 2009.
[16] D. Ricci, D. Iraji, A. Cremona, I. Furno, Proc. 39th EPS Conference on Plasma Physics, 26 July 2012, Stockholm, Sweden, 36F ECA, 2012.
[17] R. Caniello, A. Uccello, F. Ghezzi, D. Minelli, Nucl. Mater. Energy 10 (2017) 9.
[18] W. Eckstein, R. Preuss, J. Nucl. Mater. 320 (2003) 209.
[19] R. Behrisch, W. Eckstein, Sputtering by Particle Bombardment, Springer-Verlag, Berlin, 2007.
[20] S. Brezinsek, D. Borodin, J.W. Coenen, D. Kondratjew, Phys. Scr. T145 (2011) 014016.
[21] M.W. Reeks, D. Hall, J. Aerosol Sci. 32 (2001) 1.
[22] G. Ziskind, Rev. Chem. Eng. 22 (2006) 1.
[23] L. Vitos, A.V. Ruban, H.L. Skriver, J. Kollar, Surf. Sci. 411 (1998) 186.
[24] V.A. Parsegian, Van der Waals forces, Cambridge University Press, Cambridge, 2006.
[25] J.N. Israelachvili, Intermolecular and Surface Forces, Academic Press, New York, 2011.
[26] Y. Ueda, J.W. Coenen, G. De Temmerman, R.P. Doerner, Fusion Eng. Des. 89 (2014) 901.
[27] M. Oberkofler, G. Meisl, A. Hakola, A. Drenik, Phys. Scr. T167 (2016) 014077.
[28] G. De Temmerman, T. Hirai, R.A. Pitts, Plasma Phys. Control. Fusion 60 (2018) 044018.
[29] C.H. Skinner, C.A. Gentile, L. Ciebiera, S. Langish, Fusion Sci. Technol. 45 (2004) 11.
[30] J. Winter, Phys. Plasmas 7 (2000) 3862.